Electron beam dynamics in combined guide and pump magnetic fields for free electron laser applications

L. Friedland

Department of Computer Science, Yale University, New Haven, Connecticut 06520
(Received 13 December 1979; accepted 21 August 1980)

The propagation of a cold relativistic electron beam in a free electron laser with an axial guide magnetic field is considered. The possibility of several steady-state helical trajectories for the electrons is shown, and the stability against perturbations and accessibility of such steady states is considered. Necessary and sufficient conditions for the stability are derived and indicate the importance of the transition region at the entrance of the laser. Possible modes of operation of the laser in different steady-state regimes are suggested and illustrated by numerical examples.

I. INTRODUCTION

The propagation of a relativistic electron beam in transverse periodic magnetic structures has been studied extensively in recent years. These studies were stimulated by the first experimentally successful free electron laser[1] which confirmed the theoretically predicted[2] possibility of using the energy stored in the relativistic beam as a source of short wavelength coherent radiation.

The most frequently used periodic magnetic pump field in a free electron laser is the transverse field produced on the axis of a double helical current winding with equal and opposite currents in each helix (a device usually referred to as a magnetic wiggler). The unperturbed motion of the electrons of the beam in the wiggler is quite simple. The reason for simplicity is that the magnetic field on the axis of a wiggler can be approximately described by a transverse vector potential $\mathbf{A}_\perp(z)$, depending only on the distance z along the axis. Therefore, the canonical transverse momentum $\mathbf{P}_\perp = \gamma m \mathbf{v}_\perp - (e/c)\mathbf{A}_\perp$ of an electron is a constant of motion,[3] which with the conservation of energy $\gamma = [1 - (v_\perp/c)^2 - (v_\parallel/c)^2]^{-1/2} = \text{const}$, uniquely defines the perpendicular and parallel components $\mathbf{v}_\perp$ and $\mathbf{v}_\parallel$ of the velocity of the electrons in the beam, for a given assignment of $\mathbf{A}_\perp(z)$. It can now be easily shown[4] that the electrons in a magnetic wiggler have helical trajectories with the same period as that of the wiggler. This simple model of the motion has been exploited in many theoretical studies, describing the operation and parametric behavior of the free electron laser.[5]

In all experiments, however, there is also an axial guide magnetic field.[1,6,7] This, of course, increases the number of parameters characterizing the free electron laser, but at the same time introduces greater complexity into the theory. The vector potential is now dependent on x and y and the perpendicular canonical momentum $\mathbf{P}_\perp$ is no longer a constant of motion; as a result, in general, no simple analytic solution for the electron trajectories can be found. Although so called "steady-state" helical trajectories with the same period as that of the wiggler and constant values of $|\mathbf{v}_\perp|$ and $|\mathbf{v}_\parallel|$ are allowed by the system, they cannot be obtained with arbitrary inlet conditions in the electron beam. Nevertheless, these are the trajectories usually used in the theory,[4,8] without studying the problem of how the steady-state situation can be achieved. An additional complication with the presence of an axial magnetic field is that, as will be shown in Sec. II of this paper, in general, there exist several possible steady-state trajectories for the same values of the axial field and wiggler parameters, and the question arises as to which of these states is accessible with given inlet conditions of the electron beam. Thus, in the presence of an axial guide field the initial conditions and the structure of the transition region at the entrance of the free electron laser may be of crucial importance in regard to the possible modes of operation of the device. These factors become even more important if the idea of recycling[9] is applied, and the electrons are forced to pass the transition region many times.

This paper presents a study of these important questions. In Sec. II, we derive the possible steady states in the homogeneous part of a free electron laser and study the stability of these states to perturbations of electron velocities. The transition region is included in the theory in Sec. III, where the possible ways of operating a free electron laser in different steady states are suggested and illustrated by numerical examples.

II. EQUATIONS OF MOTION AND STABILITY

Consider a cold relativistic electron beam moving in a magnetic field of the form

$$\mathbf{B} = \hat{B}(z)\mathbf{e}_z + \nabla \times \mathbf{A}\,, \tag{1}$$

where

$$\mathbf{A} = -\hat{A}(z)[\mathbf{e}_x \cos\phi(z) + \mathbf{e}_y \sin\phi(z)]\,, \tag{2}$$

and

$$\phi = \int_0^z k_0(z')\,dz'\,. \tag{3}$$

For $\hat{A}$ and k_0 independent of z, the vector potential (2) describes the field on the axis of an infinite magnetic wiggler, where, as is well-known[10]

$$\hat{A} \propto I[\rho k_0 K_0(\rho k_0) + K_1(\rho k_0)]\,, \tag{4}$$

where I is the current in the wiggler, ρ is its radius, $k_0 = 2\pi/\lambda_0$, λ_0 is the pitch of the winding of the wiggler, and $K_{0,1}$ are the modified Bessel functions of the second kind. By using the more general form (2) for the vector

 0031-9171/80/122376-07$00.90

potential, we have in mind primarily the possibility of slow variations of the wiggler parameters ρ and k_0 with z, and assume that in this case the magnitude $\hat{A}(z)$ in (2) can be approximated by expression (4), where ρ and k_0 correspond to the values of these parameters in the nonuniform wiggler at point z.

Although the magnetic field represented by the potential (2) does not satisfy $\nabla \times \mathbf{B} = 0$, it gives a good approximation of the exact curl-free field on an infinite wiggler at small distances r from its axis. Indeed, as was shown in Ref. 4, the relative deviation of the transverse component of the field from that described by (2) is of the order of $(k_0 r)^2$. Accordingly, if the beam radius l is such that $(k_0 l)^2 \ll 1$, the actual transverse field can be well represented by Eq. (2). The axial component of the field of a wiggler near the axis grows[4] as $k_0 r$; it can be neglected, however, in the presence of a strong axial guide field. We will also limit ourselves to low current beams so that the influence of the self-space charge on the beam can be neglected. We thus require that the transverse electrostatic field be much smaller than $v_\parallel B_\perp / c = v_\parallel k_0 \hat{A}/c$, or, assuming axial symmetry of the beam, $\omega_p^2 r \ll 2ek_0 \hat{A} v_\parallel / mc$, where ω_p is the plasma frequency. If, for example, $r = 0.3$ cm, $B = 500$ G, and $v_\parallel \simeq c$, the maximum current density allowed by the model will be approximately 250 A/cm^2. The small signal gain in a free electron laser at these conditions, however, may be substantial,[11] so that the results of the present work could be important in current experiments.

We now consider the momentum equation for the electrons of the beam

$$\frac{d}{dt}(\gamma \mathbf{v}) = -\frac{e}{mc}\mathbf{v} \times \mathbf{B}, \tag{5}$$

where

$$\gamma = [1 - (v^2/c^2)]^{-1/2}. \tag{6}$$

Let

$$\begin{aligned} \mathbf{e}_1(z) &= -\mathbf{e}_x \sin\phi + \mathbf{e}_y \cos\phi, \\ \mathbf{e}_2(z) &= -\mathbf{e}_x \cos\phi - \mathbf{e}_y \sin\phi, \\ \mathbf{e}_3(z) &= \mathbf{e}_z. \end{aligned} \tag{7}$$

Then, the cononical model vector potential is

$$\mathbf{A} = \hat{A}(z)\mathbf{e}_2, \tag{8}$$

and

$$\mathbf{B} = \hat{B}(z)\mathbf{e}_3 - \frac{d\hat{A}}{dz}\mathbf{e}_1 - k_0 \hat{A}\mathbf{e}_2. \tag{9}$$

On expressing the velocity v in terms of the orthogonal vectors $\mathbf{e}_1$, $\mathbf{e}_2$, and $\mathbf{e}_3$ and using

$$\frac{d\mathbf{e}_1}{dt} = k_0 v_3 \mathbf{e}_2; \quad \frac{d\mathbf{e}_2}{dt} = -k_0 v_3 \mathbf{e}_1, \tag{10}$$

one can rewrite (5) as

$$\begin{aligned} \gamma \frac{dv_1}{dt} &= \gamma k_0 v_2 v_3 - \frac{e}{mc}(v_2 \hat{B} + k_0 v_3 \hat{A}), \\ \gamma \frac{dv_2}{dt} &= -\gamma k_0 v_1 v_3 + \frac{e}{mc}\left(v_1 \hat{B} + v_3 \frac{d\hat{A}}{dz}\right), \\ \gamma \frac{dv_3}{dt} &= \frac{e}{mc}\left(k_0 v_1 \hat{A} - v_2 \frac{d\hat{A}}{dz}\right). \end{aligned} \tag{11}$$

On using normalized velocities $u_i = v_i/c$ and "time" $\tau = ct$ and defining $\xi(z) = e\hat{A}/mc^2$ and $\Omega = e\hat{B}/mc^2$, one can write (11) in the form

$$\dot{u}_1 = u_2\left(k_0 u_3 - \frac{\Omega}{\gamma}\right) - \frac{k_0 \xi}{\gamma} u_3, \tag{12}$$

$$\dot{u}_2 = -u_1\left(k_0 u_3 - \frac{\Omega}{\gamma}\right) + \frac{1}{\gamma}\frac{d\xi}{dz} u_3, \tag{13}$$

$$\dot{u}_3 = \frac{k_0 \xi}{\gamma} u_1 - \frac{1}{\gamma}\frac{d\xi}{dz} u_2. \tag{14}$$

First consider the homogeneous case, where $\Omega = \Omega_0 = \text{const}$, $k_0 = \text{const}$, and $\xi = \xi_0 = \text{const}$. In this case, Eqs. (12)–(14) have a particular solution

$$u_{10} = 0, \quad u_{30} = \text{const},$$

and

$$u_{20} = \frac{k_0 \xi_0 u_{30}/\gamma}{k_0 u_{30} - \Omega/\gamma}, \tag{15}$$

which with the conservation of energy

$$1/\gamma^2 = 1 - u_{20}^2 - u_{30}^2 \tag{16}$$

defines the values of u_{20} and u_{30}. The question arises as to how this steady-state solution can be achieved. One can answer this question only by considering the transition region of the wiggler, where ξ and k_0 may depend on z. Here, one would expect that for initial conditions in the beam $u_1 = u_2 = 0$, when the vector potential ξ grows slowly enough with z, the velocities u_2 and u_3 would gradually approach their steady-state values u_{20} and u_{30}, and at the same time u_1 remains zero. It can be shown, however, that, in general, this cannot be the case. In fact, one gets from (13) that if $u_1(z) \equiv 0$,

$$\dot{u}_2 - \frac{1}{\gamma}\frac{d\xi}{dz} u_3 = u_3 \frac{d}{dz}\left(u_2 - \frac{\xi}{\gamma}\right) = 0, \tag{17}$$

and therefore $u_2 = \xi/\gamma$, which, on using (12), requires that $\Omega(z) \equiv 0$. Thus, in the presence of an axial magnetic field and for the initial conditions on u considered here, u_1 cannot remain zero in the transition region. The maximum that can be expected is that the component u_1 in the transition region remains small in comparison with u_2 and u_3. When this is the case, and, in addition, u_1 remains small as the beam propagates in the homogeneous part of the wiggler we define the beam to be *stable* and now proceed to the study of this special kind of stability.

First, consider the homogeneous region of the device and in this region let

$$u_1(\tau) = w_1(\tau), \quad u_2(\tau) = u_{20} + w_2(\tau), \quad u_3(\tau) = u_{30} + w_3(\tau), \tag{18}$$

where u_{20} and u_{30} are given by (15) and (16), and $w_i(\tau)$ are small perturbations to the steady-state solution. Then, on linearizing Eqs. (12)–(14) one gets

$$\dot{w}_1 = a w_2 + b w_3, \tag{19}$$

$$\dot{w}_2 = -a w_1, \tag{20}$$

$$\dot{w}_3 = c w_1, \tag{21}$$

where

$$a = k_0 u_{30} - \frac{\Omega}{\gamma} = \frac{k_0 \xi_0}{\gamma} \frac{u_{30}}{u_{20}}, \tag{22}$$

$$b = k_0 u_{20} - \frac{k_0 \xi_0}{\gamma} = \frac{\Omega}{\gamma} \frac{u_{20}}{u_{30}}, \tag{23}$$

$$c = k_0 \xi_0 / \gamma . \tag{24}$$

Equation (19) then gives

$$\ddot{w}_1 = a\dot{w}_2 + b\dot{w}_3 = -(a^2 - bc) w_1 . \tag{25}$$

Thus, the necessary condition for the stability of the electron beam is

$$a^2 - bc > 0 , \tag{26}$$

or

$$\frac{\Omega}{k_0 \xi_0} \left(\frac{u_{20}}{u_{30}} \right)^3 < 1 . \tag{27}$$

Further study of the stability problem must involve a knowledge of u_{20} and u_{30}. Let us combine Eqs. (15) and (16); there results

$$1 - u_{30}^2 - \left(\frac{\xi}{\gamma} \right)^2 \frac{u_{30}^2}{(u_{30} - \Omega/\gamma k_0)^2} = \frac{1}{\gamma^2} . \tag{28}$$

This equation can be rewritten in the form

$$F = F_1 - F_2 = 0 , \tag{29}$$

where

$$F_1 = \frac{1 - 1/\gamma^2}{u_{30}^2} , \tag{30}$$

and

$$F_2 = 1 + \frac{(\xi_0/\gamma)^2}{(u_{30} - \Omega/k_0\gamma)^2} . \tag{31}$$

Assuming $(\xi_0/\gamma)^2 < 1 - 1/\gamma^2$ for γ large enough, the functions F_1 and F_2 have the general form shown in Fig. 1 for various values of Ω. It can be seen from Fig. 1(a) that for $\Omega = 0$, there are two solutions for u_{30}, corresponding to different directions of propagation of the

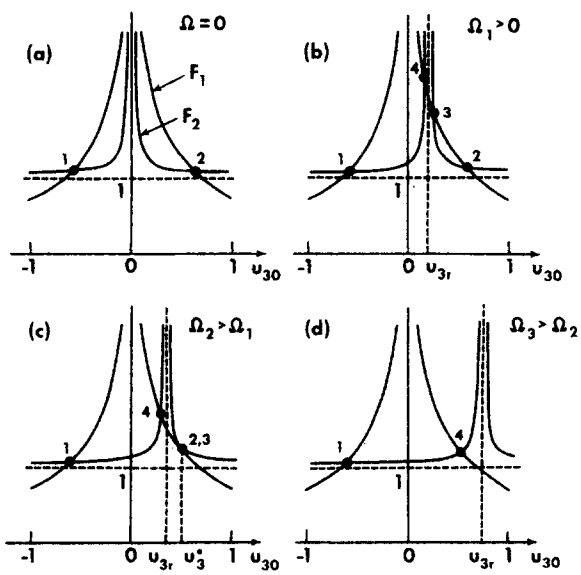

FIG. 1. Schematic of the functions F_1 and F_2, defining various possible steady-state solutions for u_{30}.

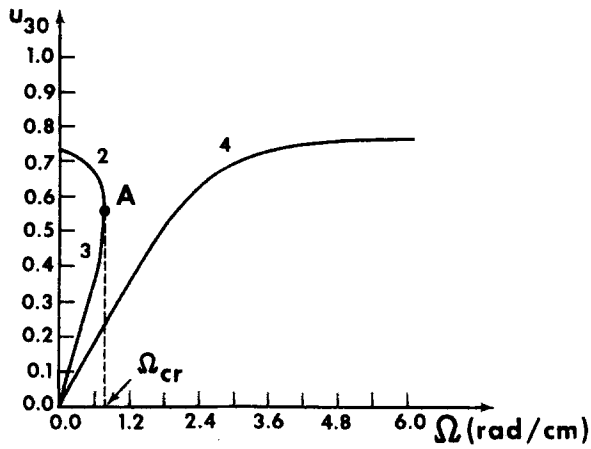

FIG. 2. The real positive branches of u_{30} vs the cyclotron frequency Ω, characterizing the guide magnetic field.

electron beam. In the presence of a weak axial magnetic field, there exist two additional solutions for u_{30} adjacent to the resonance velocity $u_{3r} = \Omega/k_0\gamma$, as shown in Fig. 1(b). If one continues to increase Ω, a situation is reached, where again there remain only two real solutions for u_{30} [Figs. 1(c), (d)]. The diagram, where all possible real positive branches of u_{30} are presented as a function of Ω, is given in Fig. 2 for a sample case in which $\gamma = 1.587$, $k_0 = 1.5708$ cm^{-1}, and $\xi_0 = 0.3873$.

Let us now find the frequency Ω_{cr} at which the roots 2 and 3 on Fig. 2 become complex. This transition corresponds to the point A on the figure. One can find Ω_{cr} by observing that the function F in Eq. (29) has only one bounded maximum at the point u_3^*, such that $F'(u_3^*) = 0$, or

$$u_3^* = \frac{\Omega}{\alpha k_0 \gamma} , \tag{32}$$

where

$$\alpha = 1 - \left(\frac{(\xi_0/\gamma)^2}{1 - 1/\gamma^2} \right)^{1/3} . \tag{33}$$

It is now clear that when F has four real roots, they are contained in the following intervals: $[-1, 0]$, $[0, u_{3r}]$, $[u_{3r}, u_3^*]$, $[u_3^*, +1]$. On the ends of these intervals the function F changes its sign, which makes it easy to find the four roots numerically. It is also clear that the roots in the last two intervals become complex, when $F(u_3^*) = 0$. Simple algebra then leads to the following expression for Ω_{cr}:

$$\Omega_{cr} = k_0 \gamma \alpha^{3/2} \left(1 - \frac{1}{\gamma^2} \right)^{1/2} . \tag{34}$$

Considering our sample case shown in Fig. 2, Eq. (34) gives the value $\Omega_{cr} = 0.763$ rad/cm.

We now return to the question of stability. It is clear that inequality (27) (which is the necessary condition for the stability) is satisfied for branch 4 in Fig. 2, since, according to (15), u_{20} is negative on this branch. Simple analysis also shows that branch 2 is stable, since the left-hand side of (27) on this branch reaches its maximum value of 1 only at $\Omega = \Omega_{cr}$; branch 3, in contrast, is always unstable.

III. TRANSITION REGION

The inequality (27) is a necessary condition for stability of the electron beam in the homogeneous part of free electron laser. This condition becomes sufficient if the electron beam enters the homogeneous region with small enough component u_1 in its velocity. We now proceed to the study of the transition region, where as will be shown, special experimental steps must be taken in order to get a stable electron beam, corresponding to various branches on the diagram on Fig. 2. Let us assume that the vector potential ξ in the transition region is a slowly growing function of z. Experimentally, this would be the case, for example, if one gradually decreases the radius ρ of the wiggler, or increases the pitch length $\lambda_0 = 2\pi/k_0$ at the end of the device as can be seen from Eq. (4). Following the ideas used in the previous section, one can find approximate solutions of (12)–(14) by using expansions (18), where u_{20} and u_{30} are now functions of z and correspond to the components of the velocity in the homogeneous case with parameters such as those at the point z in the transition region. Then, similar to (19)–(21) one has

$$\dot{w}_1 = aw_2 + bw_3 , \tag{35}$$

$$\dot{w}_2 = -aw_1 + fu_{30} , \tag{36}$$

$$\dot{w}_3 = cw_1 - fu_{20} , \tag{37}$$

where a, b, and c are given by (22)–(24) and

$$f = \frac{1}{\gamma}\frac{d\xi}{dz} . \tag{38}$$

Taking the time derivative of Eq. (35) and assuming that the coefficients a and b are slowly varying functions of z, one gets the following equation

$$\ddot{w}_1 = a\dot{w}_2 + b\dot{w}_3 + \dot{a}w_2 + \dot{b}w_3 \simeq a\dot{w}_2 + b\dot{w}_3$$
$$= -(a^2 - bc)w_1 + f(au_{30} - bu_{20}) , \tag{39}$$

or, on using (22)–(24)

$$\ddot{w}_1 = -\mu^2 w_1 + g , \tag{40}$$

where

$$\mu^2 = a^2 - bc , \tag{41}$$

and

$$g = \mu^2 \frac{u_{20}\gamma}{k_0\xi} f . \tag{42}$$

Assuming that μ is a slowly varying function of τ one can approximate the solution of the homogeneous equation

$$\ddot{w}_1 = -\mu^2 w_1 , \tag{43}$$

by the WKB solution

$$w_1(\tau) = \mu^{-1/2}[C_1 \cos\psi(\tau) + C_2 \sin\psi(\tau)] , \tag{44}$$

where

$$\psi = \int_0^\tau \mu(\tau')\, d\tau' . \tag{45}$$

Then, it can be easily shown, using the method of variation of constants in (44), that the solution of the inhomogeneous equation (40), with the initial conditions $w_1|_0 = \dot{w}_1|_0 = 0$, can be expressed as

$$w_1(\tau) = \frac{1}{\mu^{1/2}(\tau)} \int_0^\tau \frac{g(\tau')}{\mu^{1/2}(\tau')} \sin[\psi(\tau) - \psi(\tau')]\, d\tau' . \tag{46}$$

Thus, if the vector potential ξ grows slowly in the transition region (the function $f = 1/\gamma\, d\xi/dz$ is small enough), one expects the electron beam to enter the homogeneous part of the wiggler with a small magnitude of w_1, which is sufficient for the stability of the beam in this region if the inequality (27) is satisfied.

In such an adiabatic case, one can also find the trajectories of the electrons passing the transition region. Expressing the radius vector $\mathbf{r}$ of the electrons in the beam in terms of the unit vectors $\mathbf{e}_1$, $\mathbf{e}_2$, and $\mathbf{e}_3$ [see Eq. (7)], one has

$$\mathbf{r} = r_1\mathbf{e}_1 + r_2\mathbf{e}_2 + z\mathbf{e}_3 , \tag{47}$$

which on differentiation with respect to τ gives

$$\dot{\mathbf{r}} = (\dot{r}_1 - k_0u_3r_2)\mathbf{e}_1 + (\dot{r}_2 + k_0u_3r_1)\mathbf{e}_2 + \dot{z}\mathbf{e}_3 , \tag{48}$$

and therefore the trajectories are described by

$$\dot{r}_1 = u_1 + k_0u_3r_2 , \quad \dot{r}_2 = u_2 - k_0u_3r_1 . \tag{49}$$

This system of equations can be solved in the following way: Let

$$R = r_1 + ir_2 , \quad U = u_1 + iu_2 . \tag{50}$$

Then, on multiplying the second equation in (49) by i and adding it to the first equation, one gets

$$\dot{R} = U - ik_0u_3R . \tag{51}$$

If one splits R into two parts

$$R = R_0 + R_1 , \tag{52}$$

where

$$iR_0 = U/k_0u_3 , \tag{53}$$

and R_1 is assumed to be small, then on linearization in Eq. (51),

$$\dot{R}_1 = -\dot{R}_0 - ik_0u_3R_1 . \tag{54}$$

The solution of this equation for R_1 is given by

$$R_1 = -\int_0^\tau \dot{R}_0(\tau') \exp(-i\{\phi[z(\tau)] - \phi[z(\tau')]\})\, d\tau' , \tag{55}$$

where ϕ is defined by (3). Thus, if the velocities u_1, u_2, and u_3 are slowly varying functions in the transition region, R_1 remains small along the trajectories and $R \simeq R_0$, or

$$r_1(z) \simeq \mathrm{Re}(R_0) \simeq \frac{u_{20}(z)}{k_0(z)u_{30}(z)} , \tag{56}$$

$$r_2(z) \simeq \mathrm{Im}(R_0) \simeq -\frac{u_{10}(z)}{k_0(z)u_{30}(z)} \ll r_1(z) , \tag{57}$$

and therefore the electrons in this case are moving on helical orbits with adiabatically changing radius r_1, and the pitch period as that of the wiggler.

Thus, we have shown that, in principle, one can obtain a stable electron beam in a free electron laser if the variations of the parameters of the wiggler in the transition region are slow enough. This conclusion,

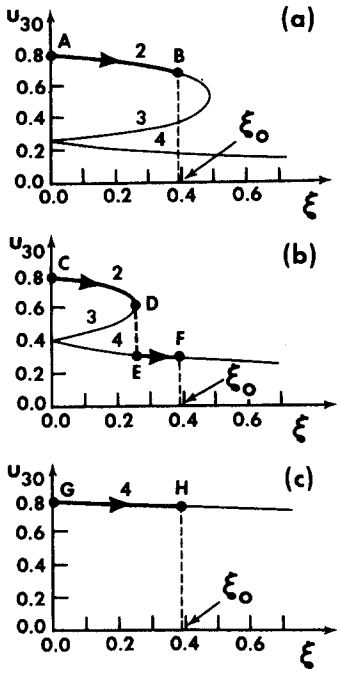

FIG. 3. The real positive branches of u_{30} vs ξ. (a) $\Omega = 0.6$ rad/cm; (b) $\Omega = 1.0$ rad/cm; (c) $\Omega = 4.0$ rad/cm.

however, is based on the approximate solution (46) for w_1 and one has to check whether all the assumptions, used in the derivation of this solution, are correct. One of these assumptions was the slowness of variation of the coefficients a and b in (35) as the beam propagates through the transition region. Let us show now that, in general, this is not guaranteed even if ξ varies slowly. The reason is that the real solutions for u_{20} and u_{30}, which are used in the definitions of a and b, do not always behave continuously. We demonstrate such a possibility in Fig. 3. In this figure, one can see the diagrams of the possible real positive solutions for u_{30}, obtained in a fashion similar to the diagram in Fig. 2, but for constant values of Ω and varying ξ. Our sample case parameters $\gamma = 1.587$ and $k_0 = 1.5708$ were again used in these graphs. As mentioned previously, the variation of ξ with constant value of k_0 can be experimentally obtained by varying the radius of the wiggler winding in the transition region, holding the pitch length $\lambda_0 = 2\pi/k_0$, constant. In Figs. 3(a,b), we show two cases with the values of Ω higher and lower than the critical value Ω_{cr} in the homogeneous region [Ω_{cr} is defined by Eq. (34), and in our sample case is equal to 0.763 rad/cm]. For $\Omega < \Omega_{cr}$, as ξ increases in the transition region, one follows the path AB in Fig. 3(a) and passes continuously to the homogeneous region corresponding to the point B on the diagram (at this point $\xi = \xi_0$). The beam is stable in this case. In contrast, if Ω is larger than Ω_{cr}, one arrives in the transition region at the point D [see Fig. 3(b)], where the branches 2 and 3 of u_{30} become complex and the homogeneous region can be only reached on the diagram by the discontinuous path DEF. The jump DE in u_{30} leads to the fast variation on the right-hand side of Eq. (12), which cannot remain small anymore, and u_1 grows in amplitude, leading to the instability of the beam. For sufficiently large values of Ω, one can again return to the stable regime. In fact, if $u_{3r} = \Omega/\gamma k_0 > 1$,

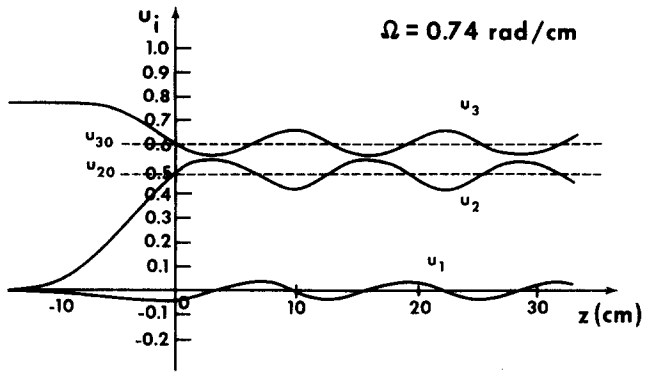

FIG. 4. The z dependence of various components of the electron velocities for $\Omega = 0.74$ rad/cm.

the only possible real branch of u_{30} is branch 4 (see Fig. 2). This situation is illustrated in Fig. 3(c). The beam follows a continuous path GH in the transition region in this case and remains stable.

In addition to these qualitative considerations, we illustrate the creation of the instability in the beam in Figs. 4 and 5, where the numerical solutions of Eqs. (12)–(14) for u_i are presented for our sample case for two values of $\Omega = 0.74$ and 0.77 rad/cm (recall that $\Omega_{cr} = 0.763$ rad/cm). We assumed in these calculations the following z dependence of the radius ρ of the wiggler winding in the transition region:

$$\rho = \begin{cases} \rho_0, & z \geq 0; \\ \rho_0 + (z/z_0)^2, & z < 0, \end{cases} \tag{58}$$

where $\rho_0 = 2.5$ cm and $z_0 = 8$ cm. The sudden transition to the unstable behavior when one goes from Fig. 4 to Fig. 5, where all the u_i's change rapidly (u_3 even becomes negative on the parts of the trajectory) is obvious.

Thus, in conclusion, if the vector potential ξ varies

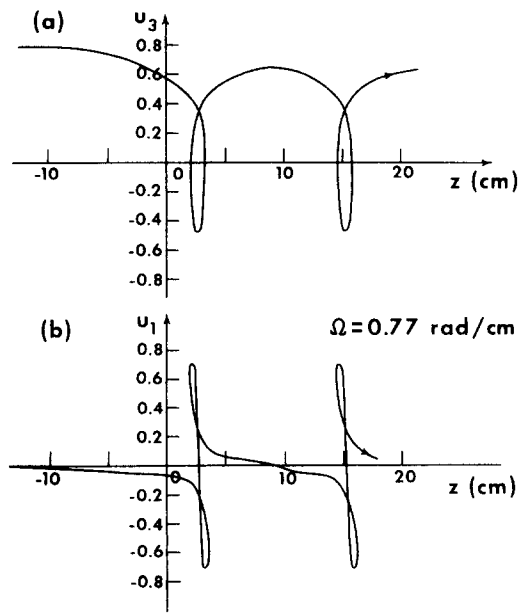

FIG. 5. The z dependence of u_1 and u_3 for $\Omega = 0.77$ rad/cm.

slowly in the transition region, one can get a stable electron beam for $\Omega < \Omega_{cr}$, and as the parameters of the wiggler vary adiabatically, the beam follows branch 2 of the possible solutions for u_{30} on Fig. 2. One can also have a stable situation for large axial magnetic fields, when branch 4 remains the only possible one for operation. One has to remember, however, that the necessary condition for the last possibility is that in the transition region $u_{3r} = \Omega/k_0\gamma > 1$. This condition can easily be satisfied when the growth of ξ in the transition region is due to the variation of the radius ρ of the wiggler, when $k_0 = \text{const}$. If in contrast, $\rho = \text{const}$ and k_0 is increasing as one approaches the end of the wiggler, larger values of the axial magnetic field are required in order to operate the device on branch 4.

Let us finally consider the question of whether it is possible with the initial conditions on the beam assumed here (namely, $u_1|_0 = u_2|_0 = 0$) to get a stable electron beam at a larger region of branch 4, especially for $u_{3r} \lesssim 1$. As mentioned before, the necessary condition (27) for stability is always satisfied on this branch, which makes it more attractive. The perpendicular component of the velocity on branch 4 can also become very large, which is again very important for possible electromagnetic wave amplification in the z direction.

The experimental scheme, which allows one to operate a free electron laser on branch 4 is shown in Fig. 6. We are exploiting the stability of the beam for large values of Ω [as demonstrated in Fig. 3(c)] and are applying a strong axial magnetic field in the transition region of the wiggler. Then, after passing this region the electrons will enter the homogeneous part of the wiggler, being on the upper part of branch 4 in Fig. 2. Now in the homogeneous region, where $\xi = \xi_0 = \text{const}$, one can gradually reduce the axial magnetic field. The beam will then follow the continuous branch 4 and one can easily reach region $\Omega \simeq \Omega_{cr}$, which was unstable with the constant axial magnetic field. We demonstrate this possibility in Fig. 7, where the solutions of Eqs. (12)–(14) are shown for exactly the same final Ω and ξ_0 as in the unstable case in Fig. 5. The same variation (58) for ρ was used in the computations. The cyclotron frequency was assumed to have the form

$$\Omega = \begin{cases} \Omega_1, & z \leq 2L, \\ (\Omega_1 - \Omega_2)e^{-(z-2L)^2/L^2} + \Omega_2, & z > 2L, \end{cases} \tag{59}$$

where $\Omega_1 = 4$ rad/cm, $\Omega_2 = 0.77$ rad/cm, and $L = 4$ cm. It can be seen from Fig. 7 that the beam remains stable and corresponds to branch 4 with negative and larger values of u_{20} than in Fig. 4, which corresponds to branch 2.

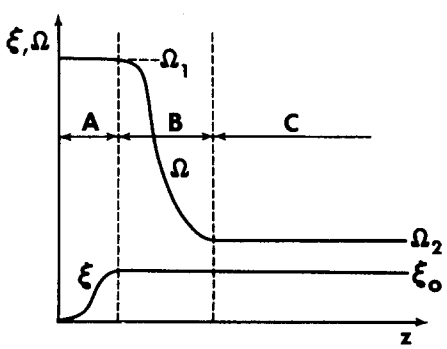

FIG. 6. Possible configuration of the pump and guide fields for operating on branch 4 of the steady-state regimes. A–transition region for ξ; B–transition region for Ω; C–homogenous part of the device.

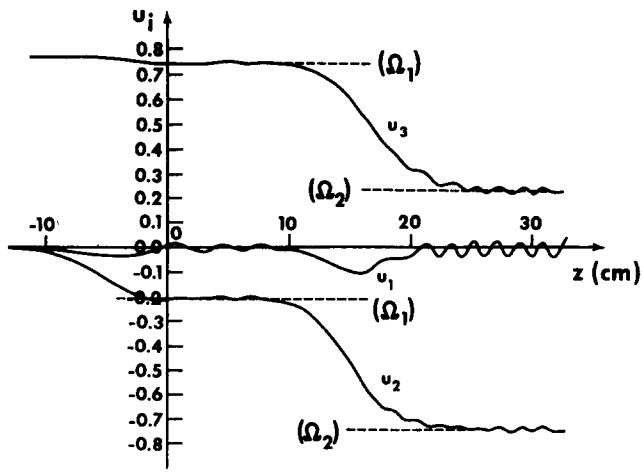

FIG. 7. The z dependence of the electron velocities in operating on branch 4 with varying guide magnetic field. $\Omega = 4$ rad/cm, $\Omega = 0.77$ rad/cm.

IV. CONCLUSIONS

(i) In operating a free electron laser with an axial magnetic field, different steady-state regimes of the helical motion of the electrons in the homogeneous part of the wiggler must be considered.

(ii) The necessary condition for the stability of these steady-state regimes is given by the inequality (27).

(iii) The transition region of a free electron laser plays an important role in determining the sufficient conditions for stability and in achieving the different modes of operation of a free electron laser for a given set of parameters of the homogeneous part of the device.

(iv) The following two models have been analyzed for operating a free electron laser in different steady-state regimes:

(a) The first is characterized by a constant axial magnetic field and gradual increase in the vector potential in the transition region. The stability of this scheme is limited by a critical value of the axial field given by Eq. (34). The value of the perpendicular component of the velocity is also limited in this steady-state regime.

(b) The second setup uses a strong axial magnetic field in the transition region. The field is then adiabatically decreased in the homogeneous part of the wiggler. This regime is always stable and can operate with any value of the axial magnetic field in the homogeneous region. The only limitation is imposed by the increasing radius of the helical trajectories of the electrons in the beam

as the perpendicular component of the velocities grows with a decrease in the axial guide field.

ACKNOWLEDGMENTS

The author wishes to express his appreciation to Professors I. B. Bernstein and J. L. Hirshfield for many useful discussions.

This work was supported in part by the Office of Naval Research and the Department of Energy.

[1]L. R. Elias, W. M. Fairbank, J. M. J. Madey, H. A. Schwettman, and T. I. Smith, Phys. Rev. Lett. 36, 717 (1976).
[2]H. Motz, J. Appl. Phys. 22, 527 (1951).
[3]I. B. Bernstein and J. L. Hirshfield, Phys. Rev. Lett. 40, 761 (1978).
[4]J. P. Blewett and R. Chasman, J. Appl. Phys. 48, 2692 (1977).
[5]Fo a review see P. Sprangle, R. A. Smith, and V. L. Granatstein, in *Infrared and Millimeter Waves*, edited by K. Button (Academic, New York, 1979), Chap. 7, p. 279.
[6]T. C. Marshall, S. Talmadge, and P. Efthimion, Appl. Phys. Lett. 31, 320 (1977).
[7]R. M. Gilgenbach, T. C. Marshall, and S. P. Schlesinger, Phys. Fluids 22, 1219 (1979).
[8]T. Kwan and J. M. Dawson, Phys. Fluids 22, 1089 (1979).
[9]L. R. Elias, Phys. Rev. Lett. 42, 977 (1979).
[10]W. R. Smythe, *Static and Dynamic Electricity* (McGraw-Hill, New York, 1950), p. 277.
[11]W. B. Colson, in *Physics of Quantum Electronics* (Addison-Wesley, New York, 1977), Vol. 5, p. 152.